Influence Of The Forming Process On The Mechanical Behavior Of A Commingled Carbon PPS Composite Part

J. Patou[1, b)], E. De Luycker[2, a)], R. Bonnaire[1, b)], T. Cutard[1, b)], G. Bernhart[1, b)]

[1]*Institut Clément Ader ICA, Université de Toulouse, MINES ALBI, Albi, France.*
[2]*Laboratoire Génie de Production LGP, Université de Toulouse, INP-ENIT, Tarbes, France.*

[a)]Corresponding author: emmanuel.de-luycker@enit.fr
[b)]{julien.patou; rebecca.bonnaire; thierry.cutard; gerard.bernhart}@mines-albi.fr

Abstract. In this research work, the influence of the forming process on commingled thermoplastic composite parts mechanical behavior was investigated. The aim of this work is to evaluate the influence of fabric shearing on the mechanical response of composite laminate. Different sheets with a given shear angle are manufactured. Tensile experimental results are compared with the properties obtained from a simple model based on the laminate plate theory for various off angles. Later, the link with a tetrahedron shape 3D part manufactured by punch deep drawing will be made.

INTRODUCTION OBJECTIVES

Influence of the forming process on the mechanical performance of a final part needs to be evaluated. After investigating the influence of void content on the mechanical behavior[5], the effect of fiber misalignment due to shear is investigated. A methodology to quantify and take into account the effect of inplane shear on the mechanical behavior of a manufactured part is introduced. Since inplane shear occurs only during the manufacturing process of 3d composite parts, during draping before high temperature consolidation, it may be difficult to extract suitable samples from the part in order to investigate this effect. In order to evaluate this influence, dedicated plates manufactured with given shear angle were manufactured. Laminate plate theory is used to estimate the behavior of the sheared plate according to the behavior of an unsheared plate. A simple model was considered for the commingled fabric layered plate behavior in membrane based on superimposed unidirectional layers contributions within the laminate plate theory. This model in compared to experimental results carried out on sheared plates with several angles.

MANUFACTURING OF SHEARED PLATES

Laminates were manufactured with 6 plies of a 5 H satin commingled semi-preg with PPS matrix and stretch-broken carbon fibers (TPFL® from Schappe Techniques). Table 1 details the fabric properties. This semi-preg was chosen because of its high formable properties and its capacity to form complex shape composite parts[2]. For all laminates, 6 plies were used with a stacking sequence [0°]6 with 0° corresponding to the warp direction of the commingled fabric.

TABLE 1. Commingled fabric properties.

Fibers	Matrix filaments	Dry fabric areal weight $[\,g/m^2\,]$	Number of plies	Volume Fiber ratio [%]	Weaving
3 K HS stretch-broken	PPS	469	6	55	5 H Satin

To establish specific and homogenous shear strains on the semi-pregs, a device based on the picture frame shearing device was developed Fig. 1(a). Plies fabrics are sheared and their edges welded with an ultrasonic welding device Fig. 1(b) to prevent any elastic springback between the shearing step and the consolidation one.

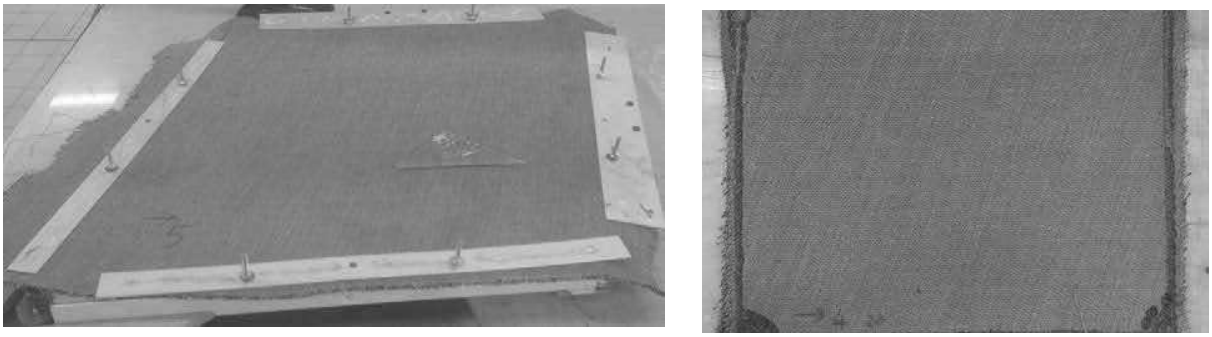

(a) (b)

FIGURE 1. Commingled fabric (specified Tab. 1) (a) during the shearing step and (b) before consolidation at 20° shear angle with an ultrasonic welding line on the edges.

A series of laminates at 0°, 10°, 20° and 30° shear angle were manufactured by autoclave consolidation. Each samples processing parameters such as processing temperature, external pressure, consolidation duration and vacuum level are reported in Tab. 2.

TABLE 2. Laminate processing cycles

Sample Id.	Shear angle	External pressure	Vacuum level	Processing Temperature	Consolidation duration
A1	0°	10 bar	-0.8 bar	310°C	25 min
A2	10°	7 bar	-0,8 bar	310°C	25 min
A3	20°	7 bar	-0,8 bar	310°C	25 min
A4	30°	7 bar	-0,8 bar	310°C	25 min

Laminates were all inspected by manual measurement of the shear angle at several locations on the surface of the plate after consolidation. Results are reported on Tab. 3.

TABLE 3. Shear angle in the laminate after consolidation

Sample Id.	Shear angle
A1	0°
A2	8.3° (+/- 0.7°)
A3	15.9° (+/- 2.1°)
A4	27.6° (+/- 1.2°)

MECHANICAL TESTING

Tensile tests were performed according to the international standards: ISO 14130 for inter-laminar shear, and ISO 155527 for tensile tests. For each laminate and direction, four specimens were tested. After consolidation, samples are water-jet cut for tensile tests in the warp, weft as well as in an intermediate direction. Orientations of the tested samples are illustrated Fig. 2.

(a) Unsheared plate (b) 16° shear angle

FIGURE 2. Traction samples orientations (a) for reference plate and (b) for plate A3.

Results obtained on the unsheared plate are used to identify the model elastic and rupture stress properties and the samples from the sheared plates are used to evaluate the validity of the model.

STRUCTURAL ASSESSMENT

X-ray tomography analysis was performed in order to get information on the laminate microstructure Fig. 4. The assessment was performed with 6 samples for each laminates in a Easytom 130 tomograph (X-Ray voltage = 44.0 kV ; source current = 173.0 µA). Scan resolution reached for this study is $10.41\ \mu m \pm 6.30x10^{-4}\ \mu m$ in all 3 directions of space.

We investigate the effect of shear angle on the void content and the geometrical characteristics of those voids: size, distribution (intra or inter yarns) as well as the orientations of the porosities. After segmentation of the data according to a threshold value on the greyscale to differentiate voids from matrix or fibers, voids morphology is represented Fig. 3. Tomography may also be used to evaluate the local shear angle in samples[1] tracking fibers orientations. In fact, porosities are of course highly influenced by the fibers directions and will be oriented along the yarns.

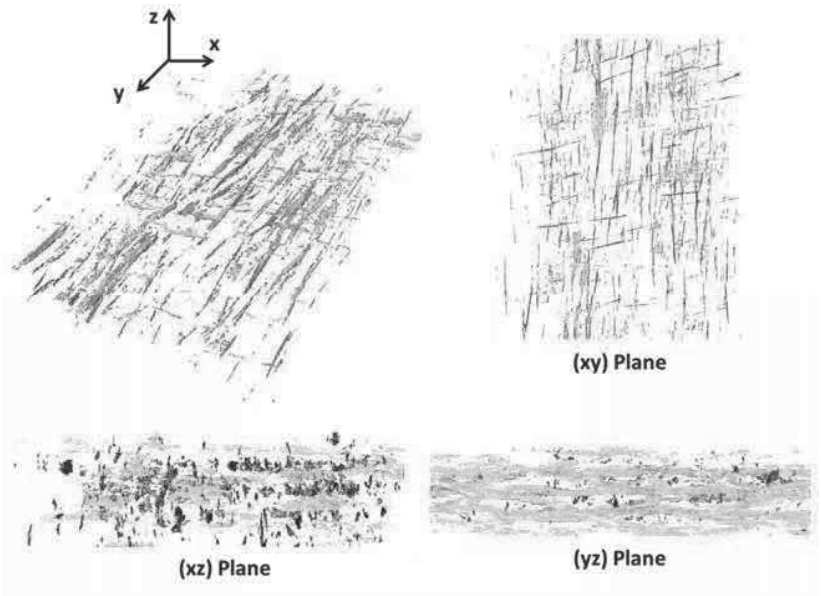

FIGURE 3. Porosity extraction from X-ray tomography analysis.

Voids levels are compared with fixed processing parameters and increasing shear angle in terms of void location, morphology and quantity. Void content results, for each shear angles, measured by CT-scan, are reported on Tab. 4. Those results are limited by the precision of the scan, but a general trend can be identified showing a decrease of the void content as the shear angle increase.

Void contents are very low for all samples (bellow 1.0%) which indicate a good consolidation level for the four laminates.

TABLE 4. Void contents in sheared plates measured by CT-scan

Sample Id.	Shear angle	Void content Average - [%]	Void content Standard deviation - [%]
A1	0°	0.55	0.19
A2	10°	0.43	0.06
A3	20°	0.20	0.08
A4	30°	0.34	0.09

For all studied samples, two void types are identified on Fig. 4:

- **Inter-voids** can be observed locally in samples. They are minor defects and are not present in the whole laminate.
- **Yarn cross failure** are observed inside warp and weft yarns Fig. 4(a). These defects, found in all laminates, are parallel to fibers directions. The phenomenon could be explained by a lack of cohesion between fibers and matrix inside yarns. However, the defect origin observed for this kind of semi-preg is not well understood.

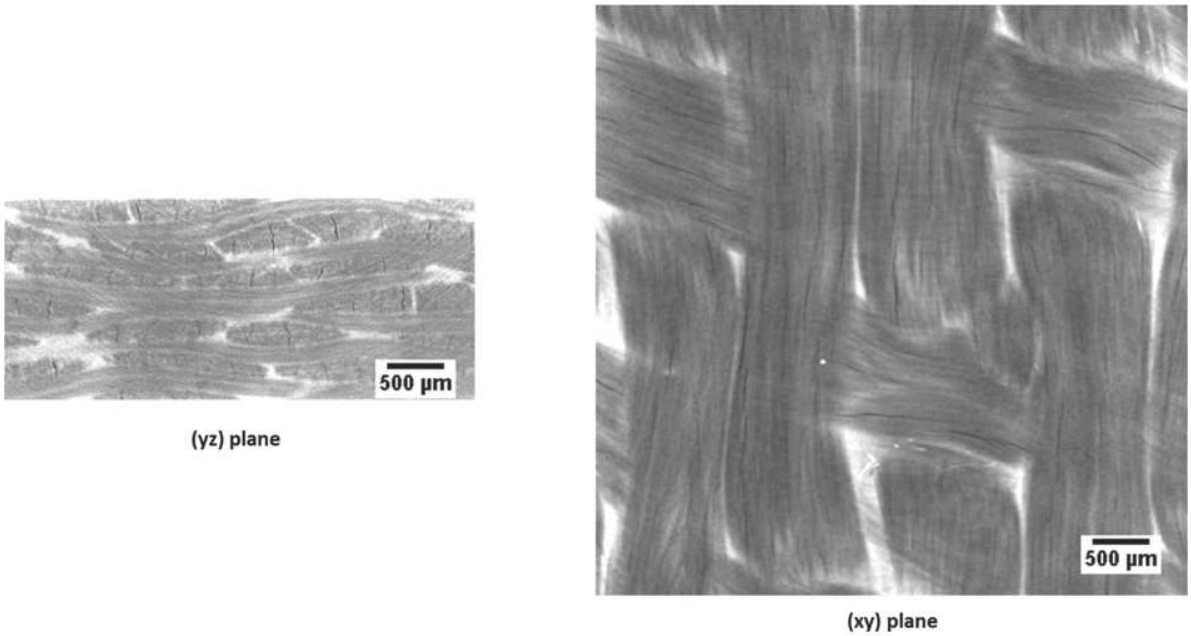

(a) (b)

FIGURE 4. Two plane images coming from sample **A3** CT-Scan

COMPARISON WITH UD LAYERS LAMINATE PLATE THEORY

The theoretical model used follows the laminate plate theory for the membrane behavior. The 6 fabric layers are modeled by 12 unidirectional layers as two networks with 90° angle for the reference plate A1, 81.3° for plate A2

and so on. Most of the elementary properties of the "UD ply" used in the model are identified with tensile tests on unsheared samples at 0°, 90° and 45° regarding stiffness, stress at failure and poison ratios as illustrated Fig. 2(a). Identified parameters are represented Tab. 5. Then, the same parameters are used with increasing shear angle. The theoretical response of the model is then compared with the experimental data measured on the sheared plates.

TABLE 5. Identified properties of the equivalent UD ply

E_l (GPa)	G_{lt} (GPa)	ν_{lt}	σ_l^t (MPa)	τ_{lt} (MPa)
85.5	3.52	0.35	625	55.5

Results are reported Tab. 6. In general the capability for the laminate plate theory to predict the Young modulus of a sheared plate is fairly good for 8° with an error between 5% and 8%, whereas the error is in the range of 20% to 35% at 16° and poor for 28° (probably due to misalignment of the fabric during cutting). Regarding failure criterion, the theory is globally conservative, overestimating Tsai-Wu criterion, but here again, if the errors are moderated for 8° shear angle, they quickly rise for the other shear angles. In conclusion, laminate plate theory is not able to predict behavior of sheared plates made out stretch-broken commingled yarns, and deeper investigations are requested to take into account the effect of these stretch broken yarns in the laminate.

TABLE 6. Comparison between the theoretical response and the experimental data

Shear angle	**8°**	**8°**	**8°**	**16°**	**16°**	**16°**	**28°**	**28°**	**28°**
Sample	0°	90°	82°	0°	90°	74°	0°	90°	62°
Expe. E (GPa)	42.6	33.8	42.4	56.0	36.5	55.8	45.9	26.1	21.4
Model E (GPa)	44.8	36.7	44.8	44.9	24.0	44.8	45.4	12.7	45.4
Tsai-Wu	1,08	0,89	1,05	1,46	1,62	1,46	0,98	1,31	0,48
Error E	5,2%	8,5%	5,5%	19,8%	34,1%	19,7%	1,1%	51,2%	111,5%
Error Tsai-Wu	8,0%	-11,0%	5,0%	46,0%	62,0%	46,0%	-2,0%	31,0%	-52,0%

In a following work, we'll compare those results with the real forming of a tetrahedral shape[3,4] in order to extract planar areas with a fixed shear angle to be tested.

ACKNOWLEDGMENTS

This work is part of ACAPULCO FUI project financed by BPI France and Midi-Pyrénées region.

REFERENCES

1. N. Q. Nguyen, M. Mehdikhani, I. Straumit, L. Gorbatikh, L. Lessard, and S. V. Lomov, "Micro-CT measurement of fibre misalignment: Application to carbon/epoxy laminates manufactured in autoclave and by vacuum assisted resin transfer moulding," *Compos. Part A Appl. Sci. Manuf.*, **104**, pp. 14–23 (2018).
2. N. Bernet, V. Michaud, P.-E. Bourban, and J.-A. . Månson, "Commingled yarn composites for rapid processing of complex shapes," *Compos. Part A Appl. Sci. Manuf.*, **32**(11), pp. 1613–1626 (2001).
3. N. Hamila, P. Boisse, F. Sabourin, and M. Brunet, "A semi-discrete shell finite element for textile composite reinforcement forming simulation," *Int. J. Numer. Methods Eng.*, **79**(12), pp. 1443–1466 (2009).
4. S. Allaoui, P. Boisse, S. Chatel, N. Hamila, G. Hivet, D. Soulat, and E. Vidal-Salle, "Experimental and numerical analyses of textile reinforcement forming of a tetrahedral shape," *Compos. Part A Appl. Sci. Manuf.*, **42**(6), pp. 612–622 (2011).
5. J. Patou, E. De Luycker, and G. Bernhart, "Influence of void content on the mechanical properties of carbon/pps laminates," in *17th European Conference on Composite Materials*, pp. 26–30 (2016).